presence of multiple limbs (for example, the two legs of *Tesnusocaris* or the leg and wing of an insect) on a single hemisegment. Modulation may occur by the regulation of the original dorsoventral position of *Dll* expression or by the migration of a subset of cells from a larger cluster (*33*). Our data are consistent with a common origin of all arthropod limbs from a more primitive structure that also expressed *Dll*. This structure was probably unjointed, like the lobopods of modern onychophorans (*1*, *34*). An examination of whether and where *Dll* is expressed in lobopods would test this view.

REFERENCES AND NOTES

1. R. E. Snodgrass, *Principles of Insect Morphology* (McGraw-Hill, New York, 1935).
2. ———, *Evolution of the Annelida, Onychophora and Arthropoda,* vol. 97 of *Smithsonian Miscellaneous Collections* (Smithsonian Institution, Washington, DC, 1938).
3. R. R. Hessler and W. A. Newman, *Fossils Strata* **4**, 437 (1975).
4. H. B. Boudreaux, *Arthropod Phylogeny with Special Reference to Insects* (Krieger, Malabar, FL, 1987).
5. J. Kukalova-Peck, *Can. J. Zool.* **70**, 236 (1992).
6. M. J. Emerson and F. R. Schram, *Science* **250**, 667 (1990).
7. D. T. Anderson, *Embryology and Phylogeny in Annelids and Arthropods* (Pergamon, Oxford, 1973).
8. S. M. Manton, *Mandibular Mechanisms and the Evolution of Arthropods* (British Museum and Queen Mary College, London, 1964), vol. 247.
9. R. E. Snodgrass, *Evolution of Arthropod Mechanisms,* vol. 138 of *Smithsonian Miscellaneous Collections* (Smithsonian Institution, Washington, DC, 1958); J. Zrzavy and P. Stys, *J. Evol. Biol.* **7**, 743 (1994).
10. S. Blair, *Bioessays* **17**, 299 (1995); S. Cohen, in *The Development of* Drosophila melanogaster, M. Bate and A. Martinez-Arias, Eds. (Cold Spring Harbor Laboratory Press, Cold Spring Harbor, NY, 1993), vol. 2, pp. 747–841; V. French and G. Daniels, *Curr. Biol.* **4**, 34 (1994); L. Held, *Bioessays* **17**, 721 (1995).
11. A. A. Simcox, I. J. H. Roberts, M. C. G. E. Hersperger, A. Shearn, J. R. S. Whittle, *Development* **107**, 715 (1989).
12. S. M. Cohen, G. Brönner, F. Küttner, G. Jürgens, H. Jäckle, *Nature* **338**, 432 (1989).
13. G. Panganiban, L. Nagy, S. B. Carroll, *Curr. Biol.* **4**, 67 (1994).
14. S. M. Cohen and G. Jürgens, *EMBO J.* **8**, 2045 (1989).
15. F. J. Diaz-Benjumea, B. Cohen, S. M. Cohen, *Nature* **372**, 175 (1994).
16. E. B. Lewis, *ibid.* **276**, 565 (1978).
17. G. Vachon *et al.*, *Cell* **71**, 437 (1992).
18. G. Struhl, *Nature* **292**, 635 (1981).
19. *Artemia* and *Mysidopsis Dll* homeodomain fragments were amplified by means of reverse transcription (RT)–PCR, essentially according to the methods of (*23*). Modifications included the use of random primers and Superscript II (Gibco-BRL) for first-strand complementary DNA (cDNA) synthesis. The 5′ and 3′ primers used to amplify the *Artemia* homeodomain encoded the amino acids Lys-Pro-Arg-Thr-Ile-Tyr and Lys-Ile-Trp-Phe-Gln-Asn, respectively; the primer sequences were 5′-CCGAATTCAARCC-NMGNACNATHTA-3′ and 5′-CCGGATCCRTTYT-GRAACCADATYTT-3′ (where R = A or G; N = A, C, G, or T; M = A or C; H = A, C, or T; Y = C or T; and D = A, G, or T). PCR conditions were 5 cycles with an annealing temperature of 43°C and 30 cycles with an annealing temperature of 50°C. PCR reaction products were cloned into the TA cloning vector (Invitrogen) and sequenced (*35*).
20. M. Beauchemin and P. Savard, *Dev. Biol.* **154**, 55 (1992).
21. M. Price, M. Lemaistre, M. Pischetola, R. Di Lauro, D. Duboule, *Nature* **351**, 748 (1991).
22. M. H. Porteus, A. Bulfone, R. D. Ciaranello, J. L. R. Rubenstein, *Neuron* **7**, 221 (1991).
23. G. W. Robinson, S. Wray, K. A. Mahon, *New Biol.* **3**, 1183 (1991).
24. N. Papalopulu and C. Kintner, *Development* **117**, 961 (1993); M. Ekker, M.-A. Akimenko, R. Bremiller, M. Westerfield, *Neuron* **9**, 27 (1992); M.-L. Dirksen, P. Mathers, M. Jamrich, *Mech. Dev.* **41**, 121 (1993); A. Simeone *et al.*, *Proc. Natl. Acad. Sci. U.S.A.* **91**, 2250 (1994).
25. The polyclonal antibody was made as follows: Rabbits were immunized 12 times over 7 months with a 200-amino acid butterfly *Dll* peptide, which comprised the homeodomain and NH_2-terminal sequences (*13*), expressed in pET23a (Novagen) with a COOH-terminal histidine tag, and purified on nickel-agarose (Novagen or Qiagen). The *Drosophila* and butterfly homeodomains are identical (*13*), yet antibodies from these animals recognized only the butterfly *Dll* protein. The antibodies therefore were not directed against the homeodomain. The rabbits were subsequently boosted with the 61–amino acid butterfly homeodomain (Fig. 1A), which was also expressed in pET23a and purified on nickel-agarose beads. After one boost with the homeodomain, the *Dll* expression pattern was observed in *Drosophila* embryos stained with crude sera. The *Dll* antibodies were affinity-purified on a column of homeodomain protein coupled to Actigel (Sterogene) and eluted with Actisep (Sterogene) (*36*).
26. M.-A. Akimenko, M. Ekker, J. Wegner, W. Lin, M. Westerfield, *J. Neurosci.* **14**, 3475 (1994); A. Bulfone *et al.*, *Mech. Dev.* **40**, 129 (1993).
27. G. Panganiban, unpublished observations.
28. A. Schrehardt, D. A. B. P. Sorgeloos, W. Decleir, E. Jaspers, Eds., Artemia *Research and Its Applications* (Universa, Wetteren, Belgium, 1987), vol. 1, pp. 5–32.
29. R. Kelsh, R. O. Weinzierl, R. A. White, M. Akam, *Dev. Genet.* **15**, 19 (1994).
30. R. W. Warren, L. Nagy, J. Selegue, J. Gates, S. Carroll, *Nature* **372**, 458 (1994).
31. M. Averof and M. Akam, *ibid.* **376**, 420 (1995).
32. N. H. Patel, personal communication.
33. B. Cohen, A. A. Simcox, S. M. Cohen, *Development* **117**, 597 (1993).
34. G. Budd, personal communication.
35. F. Sanger, S. Nicklen, A. Coulson, *Proc. Natl. Acad. Sci. U.S.A.* **74**, 5463 (1977).
36. J. Williams, J. Langeland, B. Thalley, J. Skeath, S. Carroll, in *DNA Cloning 2: Expression Systems,* D. M. Glover and B. D. Hames, Eds. (IRL Press, Oxford, 1995), pp. 15–58.
37. In situ hybridizations were carried out as described (*13*). However, *Artemia* were sonicated in phosphate-buffered saline with 0.1% Tween-20 after xylene treatment and before postfixation. Optimal sonication was determined to be the point at which 30 to 50% of the embryos were visibly disintegrated. Detailed in situ and immunostaining protocols are available on request.

38. We thank B. Rollman, J. Gates, and J. Van Stelle for handling immunizations and bleeds; J. Fallon and K. Simandl for chick embryos; N. Brown and J. Langeland for zebra fish embryos; C. Craig for spider embryos; B. Warren for centipede embryos; M. Averof for *Artemia* rearing instructions; Aquatic Research Organisms for *Mysidopsis* embryos; N. Patel and R. White for *en* and *Ubx/abdA* antibodies; K. Mahon for RT-PCR guidance; S. Paddock and L. Olds for help with figures; and J. Grenier, T. Garber, T. Williams, S. Mango, N. Patel, and anonymous reviewers for comments. Supported by an NSF–Sloan Foundation postdoctoral fellowship (G.P.) and the Howard Hughes Medical Institute (S.B.C.)

9 June 1995; accepted 13 September 1995

Selective Opioid Inhibition of Small Nociceptive Neurons

Abraha Taddese,* Seung-Yeol Nah,† Edwin W. McCleskey‡

Opioid analgesia, the selective suppression of pain without effects on other sensations, also distinguishes between different types of pain: severe, persistent pain is potently inhibited by opioids, but they fail to conceal the sensation of a pinprick. The cellular basis for this specificity was analyzed by means of patch-clamp experiments performed on fluorescently labeled nociceptive neurons (nociceptors) that innervate rat tooth pulp. Activation of the μ opioid receptor inhibited calcium channels on almost all small nociceptors but had minimal effect on large nociceptors. Somatostatin had the opposite specificity, preferentially inhibiting calcium channels on the large cells. Because persistent pain is mediated by slow-conducting, small nociceptors, opioids are thus likely to inhibit neurotransmitter release only at those primary synapses specialized for persistent pain.

Nociceptors are primary sensory neurons that are specialized to detect tissue damage and to evoke the sensation of pain (*1*). Their cell bodies are located in peripheral ganglia together with other sensory neurons, and their axons form synapses in the central nervous system that are targets for opioids (*2*). Each neuron in a sensory ganglion transduces a particular sensory modality. To be able to identify this modality in dissociated tissue culture, we fluorescently labeled nociceptors in vivo by placing crystals of a lipid soluble dye, $DiIC_{18}$, in the tooth pulp of rats. Through retrograde transport back to the cell body, $DiIC_{18}$ identifies the neurons projecting to tooth pulp (*3*). Pain is the only sensation perceived by humans when any type of physiologic stimulus is applied specifically to tooth pulp (*4*). Thus, labeling the cells that innervate tooth pulp identifies a nearly pure population of nociceptors, sensory neurons

Vollum Institute, Oregon Health Sciences University, L-474, 3181 SW Sam Jackson Park Road, Portland, OR 97201, USA.

*Present address: WEL414 Massachusetts General Hospital, Boston, MA 02114, USA.
†Present address: Veterinary School of Medicine, Chonnam National University, Kwang-Ju, South Korea.
‡To whom correspondence should be addressed.

specialized for pain perception.

Two to five days after placing a crystal of dye at the dentin-pulp border in the maxillary molars of adult rats, we dissected and dissociated the two trigeminal ganglia that contain the cell bodies of sensory neurons that innervate the face and teeth (5). Typically, 30 to 50 labeled nociceptors were obtained among the thousands of unlabeled sensory neurons in each preparation (Fig. 1). We compared cells at either end of the range of cell body diameters; the small nociceptors (≤30 μm; average, 26.4 μm) constituted about 20% of the total, and the large nociceptors (≥40 μm; average, 44.8 μm) about 25%.

We recorded current through voltage-gated Ca^{2+} and Na^+ channels with whole-cell patch clamp in labeled nociceptors with no neurite outgrowth; sustained Ca^{2+} current (I_{Ca}) amplitude was measured about 40 ms after Na^+ channels were inactivated (6). The pentapeptide (D-Ala^2,*N*-Me-Phe^4, Gly-ol)-enkephalin (DAMGO) was used to activate the μ opioid receptor, the binding site for morphine; somatostatin (somatostatin-14), which suppresses spinal nociceptive responses differently than opioids do (7), was used to activate somatostatin receptors. In a typical small nociceptor (25 μm in diameter), DAMGO (1 μM) potently inhibited I_{Ca}, whereas somatostatin (5 μM) had relatively minimal effect (Fig. 2A). In contrast to its effect on small nociceptors, DAMGO had no effect on a typical large nociceptor (45 μm in diameter), whereas somatostatin markedly inhibited I_{Ca} (Fig. 2B). Average inhibition by DAMGO (1 μM) was 21% in small nociceptors and 5% in large nociceptors (Fig. 2C). Average inhibition of I_{Ca} by somatostatin (5 μM) was 11% for small nociceptors and 30% for large nociceptors (Fig. 2D). Nociceptors of intermediate size (30 to 40 μm) differed unpredictably in their opioid and somatostatin sensitivities (Fig. 2), as did unlabeled sensory neurons of all sizes.

In addition to targeting different populations of nociceptors, DAMGO and somatostatin differed in their effective concentrations and in their time courses of Ca^{2+} channel inhibition. Half-maximal inhibition of I_{Ca} occurred at about 200 nM for DAMGO, but inhibition by somatostatin required 10 times higher concentrations (Fig. 3A). As expected, because of its local, fast signal transduction pathway (8), DAMGO inhibited Ca^{2+} channels reversibly, and there was no evidence of desensitization during exposures of several minutes (Fig. 3B); therefore, successive applications of DAMGO gave roughly identical responses. Inhibition by somatostatin was more complex. Brief applications of somatostatin caused reversible inhibition, but I_{Ca} never fully recovered after a prolonged application (Fig. 3C). After this partial recovery, subsequent applications of somatostatin diminished I_{Ca} to the previous level of inhibition, but the original, uninhibited baseline of I_{Ca} was never reached. Possibly, somatostatin inhibits I_{Ca} through two pathways: one that is reversible and one that fails to reverse in the timescale of our experiments. The differences between DAMGO and somatostatin are not caused by targeting different types of Ca^{2+} channels; both DAMGO and somatostatin inhibit N-type Ca^{2+} channels in nociceptors, as inhibition by either peptide was virtually eliminated on application of ω-conotoxin (ω-CgTx) GVIA (Fig. 3, D and E), a selective inhibitor of N channels.

Opioids inhibit "second pain," the dull ache that persists after a noxious stimulus, but they have a relatively minimal effect on "first pain," the initial sharp sensation (9).

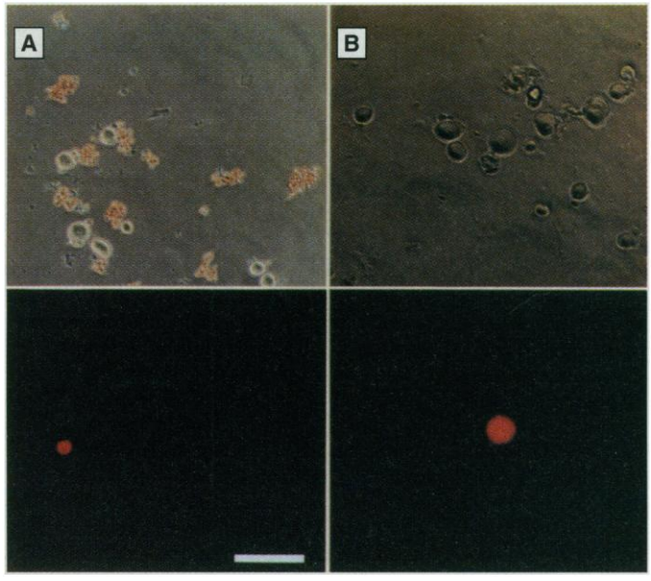

Fig. 1. Fluorescently labeled tooth pulp nociceptors in dissociated cell culture. Phase (upper) and fluorescence (lower) photographs of two fields of freshly dissociated trigeminal ganglion neurons. (**A**) Small (27 μm in diameter) nociceptor. (**B**) Large (47 μm in diameter) nociceptor. Scale bar, 100 μm. Labeled cells had diameters as small as 20 μm or as large as 60 μm, but there were more cells between 30 and 40 μm than in any other range.

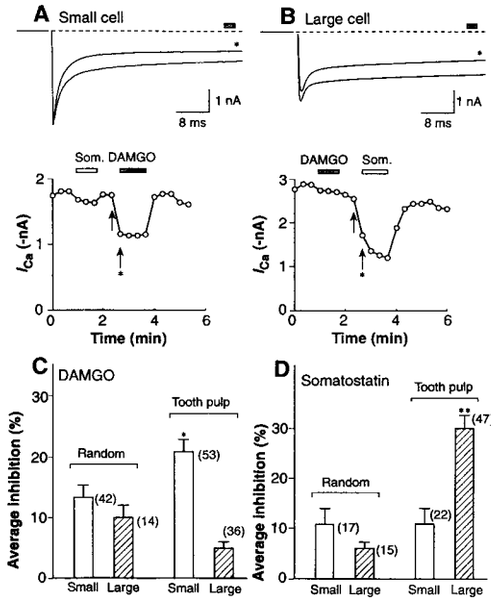

Fig. 2. Opioids and somatostatin inhibit Ca^{2+} channels in different populations of nociceptors. (**A**) DAMGO (1 μM) inhibits I_{Ca} on a small nociceptor (25 μm in diameter), but 5 μM somatostatin (Som.) has relatively minimal effect. Traces show currents evoked by pulses from −70 mV to +10 mV (100-ms duration, applied every 20 s) in the absence and in the presence (asterisk) of DAMGO; bar above the base line indicates the data points that were averaged to obtain I_{Ca} amplitude. Graph plots I_{Ca} amplitude versus time; arrows indicate data from the two traces, and bars indicate applications of somatostatin and DAMGO. As shown in previous preparations (*19*), DAMGO effects were eliminated by excess naloxone, a competitive inhibitor of opioid receptors. (**B**) The same protocol as in (A) applied to a large nociceptor (45 μm in diameter). DAMGO has no effect, but somatostatin causes marked inhibition. (**C**) Average percentage inhibition (±SEM) of I_{Ca} by 1 μM DAMGO in small (≤30 μm in diameter) and large (≥40 μm in diameter) nociceptors (Tooth pulp) and unlabeled trigeminal ganglion neurons (Random). Numbers of cells are indicated in parentheses. DAMGO caused >10% inhibition of I_{Ca} in 4 of 36 large nociceptors, and in 42 of 53 small nociceptors. (**D**) Average percentage inhibition of I_{Ca} by 5 μM somatostatin in small and large nociceptors and in unlabeled trigeminal ganglion neurons. Somatostatin caused >10% inhibition of I_{Ca} in 7 of 22 small nociceptors and in 42 of 47 large nociceptors. Ca^{2+} current was clearly inhibited (>10% decrease in amplitude) on 43% of medium-sized nociceptors tested with 1 μM DAMGO (n = 44) and on 43% tested with 5 μM somatostatin (n = 49). Asterisks in (C) and (D) indicate significant differences (paired t test; P = 0.001 for somatostatin and <0.001 for DAMGO).

The cellular mechanism for this specificity is unknown, but nociceptors may play a role because two different types of nociceptors mediate first and second pain, respectively: action potentials for first pain are transmitted by rapid-conducting, myelinated axons, and for second pain, by slow-conducting, unmyelinated axons (*10*). In teeth, shooting pain is mediated by the rapidly conducting axons, and persistent toothache by the slowly conducting axons (*11*). Because axons were severed when we dissected the neurons, we can infer axon properties only from cell body size. Cell diameter does not predict conduction velocity for medium-sized sensory neurons, but very small cells reliably have slow-conducting axons and very large cells have rapid-conducting axons (*12*). Our observations are analogous: opioid inhibition of Ca^{2+} channels is predictable for nociceptors at the extremes of cell body size, but not for medium-sized cells. Therefore, we suggest a mechanism for selective opioid inhibition of second pain: Activation of the μ opioid receptor inhibits Ca^{2+} channels predominantly on unmyelinated, slow-conducting nociceptors, thereby selectively suppressing Ca^{2+}-evoked neurotransmitter release from those presynaptic terminals subserving second pain (Fig. 4). An assay of neurotransmitter release from nociceptors might rigorously test this proposal, which presently assumes that Ca^{2+} channels at the presynaptic terminals are modulated like those at the cell body.

Selective suppression of second pain allows endogenous opioids to relieve the pain persisting from a previous injury without eliminating the awareness of immediate danger triggered by the pain of a new injury. This specificity is why opioids are typically used for postoperative pain relief but not for surgery: opioids, at analgesic doses, do not eliminate the initial sensation of a knife cut. There are a variety of anatomic locations where opioids suppress pain (*13*), and opioids modulate both Ca^{2+} and K^+ channels. Is it reasonable to suggest that opioid specificity for second pain arises solely through inhibition of Ca^{2+} channels on nociceptors? The synapse formed by nociceptors is the first synapse in the pathway for sensing pain, but it may be the final site for specificity between first and second pain because there is no evidence that their signals remain divergent at higher synapses. However, the postsynaptic membrane, where opioids activate K^+ channels (*14*), may be as important in the selective inhibition of pain as the presynaptic membrane, where opioids inhibit neurotransmitter release (*2*). The modulation of K^+ channels, which is essential to the postsynaptic action of opioids, has no presynaptic function in this case because opioids do not affect K^+ channels in sensory neurons (*15*, *16*). Evidently, the inhibition of Ca^{2+} channels, coupled with the exponential dependence of transmitter release on Ca^{2+} entry (*17*), is the primary method of presynaptic inhibition of nociceptors by opioids.

Tooth pulp innervation is complex; sensory endings contained in the tooth pulp respond to mechanical, thermal, or chemical inputs (*18*). Nevertheless, any physiologic stimulation of the pulp evokes the sensation of pain, and patients cannot distinguish between different types of stimuli (*4*). This necessarily implies that all sensory neurons innervating the pulp, despite their heterogeneity, form synapses on central neurons in the signaling pathway leading to pain perception. By providing in vitro identification of the presynaptic cell of this synapse, our preparation makes possible different cellular and molecular studies of pain and analgesia.

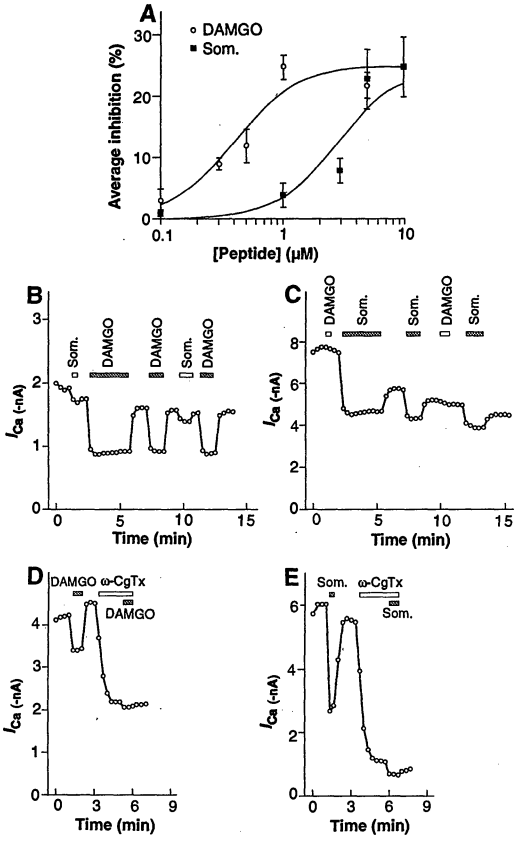

Fig. 3. Comparison of DAMGO and somatostatin modulation of I_{Ca}. (**A**) Average percentage inhibition of I_{Ca} by different concentrations of DAMGO (open symbols, averages from five cells of 25-μm mean diameter) and somatostatin (closed symbols, averages from seven cells of 44-μm mean diameter). The best least-squares fits of Hill plots (curves) having identical slope and maxima provide an estimate of concentrations for similar effects by the two peptides. (**B**) Time course of I_{Ca} amplitude with multiple applications of DAMGO (1 μM) on a representative small nociceptor. Opioid inhibition is characterized by rapid reversibility and reproducible inhibition on successive applications. On average, the increase in current on removing DAMGO after 3 min was 0.76 ± 0.04 (SEM) of the initial decrease in current with DAMGO (n = 6 cells of 27 μm mean diameter); we attribute the incomplete reversal to the rundown of I_{Ca} that inevitably occurs in 3 min. (**C**) Time course of I_{Ca} amplitude with multiple applications of somatostatin (5 μM) on a representative large nociceptor. Ca^{2+} current does not fully reverse after a 3-min application, and subsequent applications elicit a smaller, reversible inhibition. The average increase in current on removing somatostatin after 3 min was 0.41 ± 0.07 (SEM) of the initial decrease of current (n = 8 cells of 42 μm mean diameter); this is markedly less recovery than that achieved with DAMGO. (**D** and **E**) Time courses of I_{Ca} amplitude with applications of DAMGO or somatostatin before and during application of ω-conotoxin GVIA, a selective blocker of N-type Ca^{2+} channels. The toxin eliminates virtually all of the I_{Ca} that is modulated by the two peptides (n = 4 for both DAMGO and somatostatin).

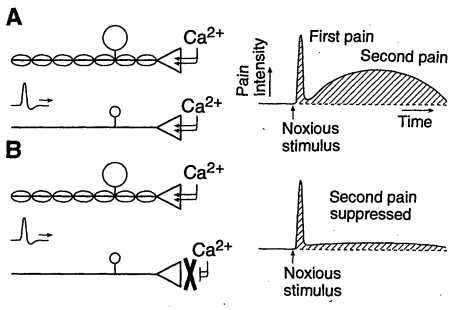

Fig. 4. Hypothesis for selective opioid inhibition of second pain. (**A**) Biphasic pain. When a noxious stimulus is applied to a distal limb, pain is perceived in two waves: first pain, the sharp, transient sensation that uses nociceptors with myelinated axons, is perceived a fraction of a second before second pain, the dull, persisting sensation that uses nociceptors with unmyelinated axons. (**B**) Opioid analgesia. By inhibiting Ca^{2+} channels only on the small, unmyelinated nociceptors, opioids diminish Ca^{2+}-evoked neurotransmitter release only from presynaptic terminals subserving second pain.

REFERENCES AND NOTES

1. P. R. Burgess and E. R. Perl, *J. Physiol. (London)* **190**, 541 (1967); H. P. Rang, S. Bevan, A. Dray, in *Textbook of Pain*, P. D. Wall and R. Melzack, Eds. (Churchill Livingstone, New York, 1994), chap. 1; H. L. Fields, *Pain* (McGraw-Hill, New York, 1987).
2. T. M. Jessel and L. L. Iverson, *Nature* **268**, 549 (1977); V. L. W. Go and T. L. Yaksh, *J. Physiol. (London)* **391**, 141 (1987).
3. M. G. Honig and R. I. Hume, *J. Cell Biol.* **103**, 171 (1986).

4. L. Edwall and L. Olgart, *Pain* **3**, 121 (1977); M. Ahlquist, L. Edwall, O. Franzen, G. Haegerstam, *ibid.* **19**, 353 (1984); U. Fors, L. Edwall, G. Haegerstam, *ibid.* **33**, 253 (1988). But also see W. K. Dong, E. H. Chudler, and R. F. Martin [*Brain Res.* **334**, 389 (1985)] for evidence of a small population of nonnociceptive neurons in cat tooth pulp.
5. A crystal of $DiIC_{18}$ (Molecular Probes, Eugene, OR) was placed in maxillary molars of male Sprague-Dawley rats (200 to 250 g) largely as described in J. L. Stephenson and M. R. Byers [*Exp. Neurol.* **131**, 11 (1995)] and in C. F. Marfurt and D. F. Turner [*J. Comp. Neurol.* **223**, 353 (1984)]. However, we drilled the crown only until a change in resistance was detected; this conservative procedure exposes the tip of the pulp chamber and results in no evident bleeding. Trigeminal ganglia were dissected 2 to 5 days after placing the dye and were dissociated as described (*16*) except for an additional centrifugation through 30% Percoll (Sigma) to remove axon debris. After dissection, the region near the tooth was checked for dye leakage. Dye leakage disqualified a preparation from use, which in fact did not occur once we became proficient with the method. Dispersed cells were resuspended in F12 growth medium, 10% fetal calf serum, and 50 ng/ml of nerve growth factor (2.5S) (Biomedical Technologies, Stroughton, MA), and plated onto glass cover slips coated with poly-D-lysine and laminin. After several hours at 37°C in 5% CO_2, cultures were transferred to L15 media (without nerve growth factor) and maintained at 4°C in air to inhibit neurite outgrowth. All cells were studied within 48 hours of dissociation. Results with freshly dissociated cells were indistinguishable from results with cells maintained in culture, which indicates that properties did not change with these culture times and conditions.
6. Sodium in the extracellular solution greatly diminished rundown of I_{Ca}. Typically, base-line I_{Ca} in neurons of all sizes was very stable for 15 min after an initial few minutes of variability (see, for example, Fig. 3B); such stability greatly facilitated comparison of modulatory effects in the cell populations. Current through Na^+ channels was not fully blocked by either tetrodotoxin or saxitoxin, so I_{Ca} amplitude was measured at least 50 ms after the onset of the pulse, when Na^+ channels were fully inactivated. A Ca^{2+} channel blocker (1 mM Cd^{2+}) applied at the end of most of the experiments confirmed that sustained current passed only through Ca^{2+} channels. The percentage of inhibition was determined by comparing I_{Ca} amplitude before drug application to amplitude 40 s after application. Solutions flowed over the cell at all times and were exchanged within seconds with an array of 1-μl pipettes. Extracellular solution consisted of 135 mM NaCl, 5 mM KCl, 1 mM MgCl, 5 mM $CaCl_2$, 10 mM Hepes, and 10 mM glucose (pH 7.3). Whole-cell pipette (intracellular) solution consisted of 100 mM CsCl, 1 mM sodium adenosine triphosphate, 0.3 mM guanosine triphosphate, 10 mM EGTA, 2.5 mM $MgCl_2$, 2 mM $CaCl_2$, 8.8 mM sodium phosphocreatine, 0.08 mM leupeptin, and 40 mM Hepes (pH 7.0) (titrated with tetraethylammonium hydroxide).
7. J. Sandkuhler, Q.-G. Fu, C. Helmchen, *Neuroscience* **34**, 565 (1990).
8. T. J. Wilding, M. D. Womack, E. W. McCleskey, *J. Neurosci.* **15**, 4124 (1995).
9. B. Y. Cooper, C. J. Vierck Jr., D. C. Yeomans, *Pain* **24**, 93 (1986); I. Jurna and G. Heinz, *Brain Res.* **171**, 573 (1979).
10. T. Lewis and E. E. Pochin, *Clin. Sci.* **3**, 67 (1937); H. Torebjork and R. G. Hallin, *Exp. Brain Res.* **16**, 321 (1972).
11. E. Jyvasjarvi and K.-D. Kniffki, *J. Physiol. (London)* **391**, 193 (1987); M. L. Ahlquist *et al.*, in *Advances in Pain Research and Therapy*, H. L. Fields, Ed. (Raven Press, New York, 1985), vol. 9, pp. 352–359.
12. A. A. Harper and S. N. Lawson, *J. Physiol. (London)* **359**, 31 (1985); K. H. Lee, K. Chung, J. M. Chung, R. E. Coggeshall, *J. Comp. Neurol.* **243**, 335 (1986).
13. A. I. Basbaum and H. L. Fields, *Annu. Rev. Neurosci.* **7**, 309 (1984).
14. T. J. Grudt and J. T. Williams, *J. Neurosci.* **14**, 1646 (1994).
15. S. A. Shefner, R. A. North, R. S. Zukin, *Brain Res.* **221**, 109 (1981); J. T. Williams and W. Zieglgansberger, *Neurosci. Lett.* **21**, 211 (1981).
16. P. T. Akins and E. W. McCleskey, *Neuroscience* **56**, 759 (1993).
17. F. A. Dodge and R. Rahamimoff, *J. Physiol. (London)* **193**, 419 (1967); R. A. Goda and C. F. Stevens, *Proc. Natl. Acad. Sci. U.S.A.* **91**, 12942 (1994).
18. M. R. Byers, *Int. Rev. Neurobiol.* **25**, 39 (1984); M. Narhi, H. Yamamoto, D. Ngassapa, T. Hirvonen, *Arch. Oral Biol.* **39**, 23S (1994).
19. E. Seward, C. Hammond, G. Henderson, *Proc. R. Soc. London Ser. B Biol. Sci.* **244**, 129 (1991); J. E. Schroeder, P. S. Fischbach, D. Zheng, E. W. McCleskey, *Neuron* **6**, 13 (1991); H. C. Moises, K. I. Ruskin, R. L. Macdonald, *J. Neurosci.* **14**, 5903 (1994).
20. We thank M. Byers, R. Goodman, A. Roos, and J. Williams for helpful critiques of an earlier version of the manuscript. Supported by the National Institute of Drug Abuse and the Lucille P. Markey Charitable Trust. A.T. received a Porter Fellowship (American Physiological Society) and participated in the Washington University–Howard Hughes Medical Institute undergraduate research program. E.W.M. received a Presidential Young Investigator Award from NSF.

16 June 1995; accepted 1 September 1995

Regulated Expression of the Neural Cell Adhesion Molecule L1 by Specific Patterns of Neural Impulses

Kouichi Itoh, Beth Stevens, Melitta Schachner, R. Douglas Fields*

Development of the mammalian nervous system is regulated by neural impulse activity, but the molecular mechanisms are not well understood. If cell recognition molecules [for example, L1 and the neural cell adhesion molecule (NCAM)] were influenced by specific patterns of impulse activity, cell-cell interactions controlling nervous system structure could be regulated by nervous system function at critical stages of development. Low-frequency electrical pulses delivered to mouse sensory neurons in culture (0.1 hertz for 5 days) down-regulated expression of L1 messenger RNA and protein (but not NCAM). Fasciculation of neurites, adhesion of neuroblastoma cells, and the number of Schwann cells on neurites was reduced after 0.1-hertz stimulation, but higher frequencies or stimulation after synaptogenesis were without effect.

Developing before the establishment of synapses, spontaneous electrical activity in prenatal neurons is of undetermined importance (*1*). Evidence suggests that impulses can regulate neuronal differentiation, but the molecular mechanisms are unknown (*1–3*). The neural cell adhesion molecule L1 has a major influence on morphogenesis of the nervous system, by regulating cell adhesion, neurite outgrowth, fasciculation, myelination, and transmembrane signaling (*4*). Possible control of L1 expression by patterned impulse activity was explored in mouse dorsal root ganglion (DRG) neurons maintained in a multicompartment cell culture preparation (Fig. 1A) (*5*), designed to deliver electrical stimulation in patterns resembling the normal impulse activity in developing sensory neurons (*1*).

Stimulation at a rate of one action potential every 10 s (0.1 Hz) reduced L1 mRNA by a factor of 12.7 ± 1.46 after 5 days of stimulation ($P < 0.001$; $n = 8$), as measured by quantitative polymerase chain reaction (PCR) (Fig. 1, C through E). Compared to 0-Hz stimulation ($n = 6$), differences were not significantly lower after 1 or 3 days of stimulation at 0.1 Hz (79 ± 11%, $n = 3$; and 89 ± 5.6%, $n = 3$). Alternative PCR strategies, with neuron-specific enolase ($n = 4$) or cyclophilin ($n = 6$) for normalization, or coamplification with the internal L1 mimic ($n = 27$) (Fig. 1B), confirmed the reduction after 5 days.

We next investigated whether regulation of L1 mRNA was sensitive to the particular pattern of impulses, as would be required to optimize structural and functional relations according to the information processing efficacy of the newly formed circuit. Stimulation at higher frequencies for 5 days (0.3 or 1 Hz; $n = 3$ and 4) (Fig. 1B) and pulsed stimulation (0.5-s, 10-Hz bursts every 2 s; $n = 2$) failed to alter levels of L1 mRNA. Chronic membrane depolarization for 5 days with 60 mM KCl was without effect ($n = 3$).

Protein immunoblot analysis showed a decrease in L1 polypeptide amounts accompanying the reduction of L1 mRNA (Fig. 2). Both molecular species of L1 in DRG neurons (210 and 230 kD) (*6*, *7*) decreased significantly after 5 days of 0.1-Hz stimulation ($P < 0.05$, $n = 21$), but not after an

K. Itoh, B. Stevens, R. D. Fields, National Institutes of Health, National Institute of Child Health and Human Development, LDN 49/5A38, Neurocytology and Physiology Unit, Bethesda, MD 20892, USA.
M. Schachner, Department of Neurobiology, Swiss Federal Institute of Technology, Honggerberg, 8093 Zurich, Switzerland.
*To whom correspondence should be addressed.